

## Onset of Transition in Mixed Convection of a Lid-Driven Trapezoidal Enclosure Filled with Water- $Al_2O_3$ Nanofluid

S. Saha<sup>1</sup>, S. Hossen<sup>1</sup>, M. H. Hasib<sup>1</sup> and S. C. Saha<sup>2</sup>

<sup>1</sup>Department of Mechanical Engineering  
Bangladesh University of Engineering and Technology, Dhaka 1000, Bangladesh

<sup>2</sup>School of Chemistry, Physics and Mechanical Engineering  
Queensland University of Technology, Brisbane QLD 4001, Australia

### Abstract

A numerical study is carried out to investigate the transition from laminar to chaos in mixed convection heat transfer inside a lid-driven trapezoidal enclosure. In this study, the top wall is considered as isothermal cold surface, which is moving in its own plane at a constant speed, and a constant high temperature is provided at the bottom surface. The enclosure is assumed to be filled with water- $Al_2O_3$  nanofluid. The governing Navier–Stokes and thermal energy equations are expressed in non-dimensional forms and are solved using Galerkin finite element method. Attention is paid in the present study on the pure mixed convection regime at Richardson number,  $Ri = 1$ . The numerical simulations are carried out over a wide range of Reynolds ( $0.1 \leq Re \leq 10^3$ ) and Grashof ( $0.01 \leq Gr \leq 10^6$ ) numbers. Effects of the presence of nanofluid on the characteristics of mixed convection heat transfer are also explored. The average Nusselt numbers of the heated wall are computed to demonstrate the influence of flow parameter variations on heat transfer. The corresponding change of flow and thermal fields is visualized from the streamline and the isotherm contour plots.

### Introduction

Mixed convection heat transfer commonly arises in many industrial applications, where both the natural and the forced convection play equally a vital role. Analysis of mixed convective flow in a lid-driven enclosure finds applications in cooling of electronic devices, lubrication technologies, heating and drying technologies [1], food processing, float glass production [2], flow and heat transfer in solar ponds, thermal hydraulics of nuclear reactors, dynamics of lakes, crystal growing, metal coating, reservoirs and cooling ponds, materials processing and among others.

Mixed convective flow in a lid-driven enclosure is generally influenced by the variation of Reynolds, Grashof and Prandtl numbers. It is expected that the heat transfer in an enclosure is naturally increased with increasing Reynolds, Grashof or Prandtl number when its respective Reynolds, Grashof or Prandtl number is kept at constant. Another important governing parameter in mixed convection is the Richardson number ( $Ri$ ) which is the ratio of Grashof number ( $Gr$ ) and the square of Reynolds number ( $Re$ ). The Richardson number can be varied by either changing  $Gr$  or  $Re$  and thus keeping one of these two parameters constant. In general, the natural convection is negligible for  $Ri < 0.1$  whereas the forced convection becomes insignificant when  $Ri > 10$  and thus mixed convection is considerable within  $0.1 \leq Ri \leq 10$ . The region at  $Ri = 1$  is considered here as the pure mixed convection regime which can be expanded from conduction dominated region to fully-developed turbulent convective flow region by varying both Grashof and Reynolds numbers simultaneously.

A numerous studies of mixed convection in lid-driven enclo-

ures with rectangular or square shapes have been reported extensively in the literature. However, in practical applications, e.g., attic spaces in building, green houses or sun drying of crops, etc., non-rectangular geometries like trapezoidal enclosures have significant impact on internal flow and temperature profiles in mixed convection. A limited numbers of previous studies have considered mixed convective flow in trapezoidal enclosures. The most popular lid-driven trapezoidal enclosure has a short stationary base wall and inclined side walls whereas the long top wall is moving in its own plane. Hossain *et al.* [3], Chowdhury *et al.* [4], Hasan *et al.* [5] and Mamun *et al.* [6] considered this type of enclosure in their studies under different thermal boundary conditions.

Recently, nanofluid plays an important role for the enhancement of heat transfer due to higher thermal conductivity of metallic nanoparticles like copper, aluminum, silver, etc., added to the mixture of base fluid such as water, ethylene glycol or propylene glycol. A large number of articles reported mixed convection heat transfer enhancement with nanofluid in regular geometries (e.g., square, rectangular or triangular enclosures). So far, no author has paid attention to the problem of mixed convection in a trapezoidal enclosure filled with nanofluid. Cheng [7] discussed the characteristics of mixed convection in a 2D lid-driven square enclosure with the variation of Richardson and Prandtl numbers. However, a similar investigation for the case of trapezoidal enclosure with the presence of nanofluid is still lacking.

The objective of the present study is to investigate the characteristics of mixed convection heat transfer in a lid-driven trapezoidal enclosure filled with water- $Al_2O_3$  nanofluid at  $Ri = 1$  by evaluating the magnitude of average Nusselt number. The values of both  $Gr$  and  $Re$  are increased gradually from the steady, laminar flow regimes to a situation where transition takes place. The presence of both plain fluid and nanofluid is also observed on the quantitative prediction of the transition phase.

### Problem Formulation

A trapezoidal enclosure of aspect ratio of  $L/H = 0.732$  is considered in the present study which is shown in figure 1 along with boundary conditions. The adiabatic side walls of the enclosure is inclined at an angle,  $\gamma = 15^\circ$ , with the vertical y-axis since Chowdhury *et al.* [4] recommended this configuration better than the lid-driven square enclosure for mixed convection heat transfer. For this configuration, the domain area of the trapezoid becomes unity relative to the area of a square of length  $H$ . The short base wall is stationary and heated at constant temperature,  $T_h$  while the long top wall is moving in its own plane at a constant speed  $u_o$  and is kept at constant surrounding temperature,  $T_c (< T_h)$ .

The working fluids (water and water- $Al_2O_3$  nanofluid) are assumed to be incompressible Newtonian fluid and their proper-

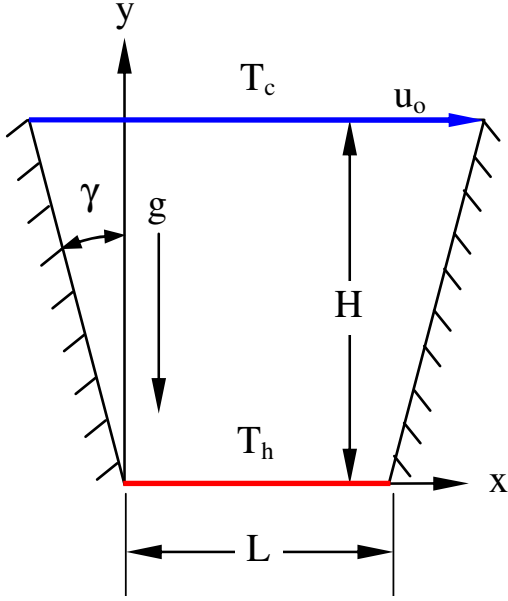


Figure 1. Schematic diagram of the trapezoidal cavity having heated wall on the short base.

ties are constant except density variation of the nanofluid with temperature according to the Boussinesq approximation. By neglecting viscous dissipation and radiation effect with no internal heat generation, the non-dimensional forms of continuity, momentum and energy equations are expressed as,

$$\frac{\partial U}{\partial X} + \frac{\partial V}{\partial Y} = 0, \quad (1)$$

$$U \frac{\partial U}{\partial X} + V \frac{\partial U}{\partial Y} = -\frac{\partial P}{\partial X} + \frac{\mu_{nf}}{\rho_{nf} \nu_{nf}} \frac{1}{Re} \left( \frac{\partial^2 U}{\partial X^2} + \frac{\partial^2 U}{\partial Y^2} \right), \quad (2)$$

$$U \frac{\partial V}{\partial X} + V \frac{\partial V}{\partial Y} = -\frac{\partial P}{\partial Y} + \frac{\mu_{nf}}{\rho_{nf} \nu_{nf}} \frac{1}{Re} \left( \frac{\partial^2 V}{\partial X^2} + \frac{\partial^2 V}{\partial Y^2} \right) + \frac{(\rho\beta)_{nf} Ri \Theta}{\rho_{nf} \beta_f}, \quad (3)$$

$$U \frac{\partial \Theta}{\partial X} + V \frac{\partial \Theta}{\partial Y} = \frac{\alpha_{nf}}{\alpha_f} \frac{1}{Re Pr} \left( \frac{\partial^2 \Theta}{\partial X^2} + \frac{\partial^2 \Theta}{\partial Y^2} \right), \quad (4)$$

where, the dimensionless parameters in the above equations are defined as,

$$X = \frac{x}{H}, Y = \frac{y}{H}, U = \frac{u}{u_o}, V = \frac{v}{u_o}, P = \frac{p}{\rho_{nf} u_o^2}, \Theta = \frac{T - T_c}{T_h - T_c}, \quad (5)$$

and the non-dimensional governing parameters can be expressed as,

$$Re = \frac{u_o H}{\nu_f}, Gr = \frac{g \beta_f (T_h - T_c) H^3}{\nu_f^2}, Pr = \frac{\nu_f}{\alpha_f}, Ri = \frac{Gr}{Re^2}. \quad (6)$$

The thermo-physical properties of the nanofluid such as effective density ( $\rho_{nf}$ ), effective viscosity ( $\mu_{nf}$ ), thermal expansion coefficient ( $\beta_{nf}$ ), effective thermal diffusivity ( $\alpha_{nf}$ ), effective thermal conductivity ( $k_{nf}$ ) and the heat capacitance of the nanofluid can be obtained from the following relations:

$$\rho_{nf} = (1 - \phi) \rho_f + \phi \rho_s, \quad (7)$$

| Property                    | Water    | Al <sub>2</sub> O <sub>3</sub> |
|-----------------------------|----------|--------------------------------|
| $C_p$ (J/kgK)               | 4179     | 765                            |
| $\rho$ (kg/m <sup>3</sup> ) | 997.1    | 3970                           |
| $k$ (W/mK)                  | 0.613    | 25                             |
| $\beta \times 10^5$ (1/K)   | 21       | 0.85                           |
| $\mu$ (Pa.s)                | 0.001003 | -                              |

Table 1. Thermo-physical properties of water and Al<sub>2</sub>O<sub>3</sub> nanoparticles [8].

| Boundary wall | Velocity       | Temperature                     |
|---------------|----------------|---------------------------------|
| Top wall      | $U = 1, V = 0$ | $\Theta = 0$                    |
| Bottom wall   | $U = V = 0$    | $\Theta = 1$                    |
| Side walls    | $U = V = 0$    | $\partial\Theta/\partial n = 0$ |

Table 2. Non-dimensional boundary conditions of the present problem.

$$\mu_{nf} = \frac{\mu_f}{(1 - \phi)^{2.5}}, \quad (8)$$

$$(\rho\beta)_{nf} = (1 - \phi)(\rho\beta)_f + \phi(\rho\beta)_s, \quad (9)$$

$$\alpha_{nf} = \frac{k_{nf}}{(\rho C_p)_{nf}}, \quad (10)$$

$$\frac{k_{nf}}{k_f} = \frac{k_s + 2k_f - 2\phi(k_f - k_s)}{k_s + 2k_f + \phi(k_f - k_s)}, \quad (11)$$

$$(\rho C_p)_{nf} = (1 - \phi)(\rho C_p)_f + \phi(\rho C_p)_s. \quad (12)$$

Here,  $\phi$  is the solid-volume fraction of the nanoparticles and the subscripts 's', 'f' and 'nf' represent the properties of nanoparticles, base fluid and nanofluid, respectively. The thermo-physical properties of the base fluid (water) and the nanoparticles (Al<sub>2</sub>O<sub>3</sub>) are presented in table 1.

The non-dimensional boundary conditions for the present problem are listed in table 2. The characteristics of mixed convection heat transfer can be assessed by evaluating the average Nusselt number of the heated bottom wall and is expressed by the following relation,

$$Nu = \frac{hL}{k_f} = -\frac{k_{nf}}{k_f} \frac{H}{L} \int_0^{L/H} \left( \frac{\partial \Theta}{\partial Y} \right)_{Y=0} dX. \quad (13)$$

## Simulation Procedure

The numerical procedure used to solve the governing equations (1–4) for the present problem follows the Galerkin finite element method which is well documented by Zienkiewicz and Taylor [9]. A non-uniform eight-noded quadrilateral mesh element is implemented in the solution domain especially adopting finer elements near the solid boundary to capture the rapid changes in the dependent variables. All eight nodes are associated with velocities as well as temperature, only the corner nodes are associated with pressure. The relative tolerance for the error criteria is considered to be  $10^{-6}$ .

## Grid Sensitivity Check

Test for the accuracy of grid sensitivity is examined for the arrangements of seven different non-uniform mesh with the following number of elements within the trapezoidal enclosure:  $50 \times 50$ ,  $60 \times 60$ ,  $65 \times 65$ ,  $70 \times 70$ ,  $75 \times 75$ ,  $80 \times 80$  and  $85 \times 85$ . The results in terms of average Nusselt number of the heated wall for constant  $Ri$ ,  $Re$  and  $Gr$  condition are shown in table 3. From these comparisons, it is clear that  $70 \times 70$  non-uniform mesh elements are sufficient to produce the optimum result. However,  $75 \times 75$  mesh is selected for the present simulation in order to attain more accuracy.

| Element numbers | Node numbers | Nu       |
|-----------------|--------------|----------|
| 50 × 50         | 43405        | 7.000399 |
| 60 × 60         | 62285        | 7.001171 |
| 65 × 65         | 73000        | 7.001416 |
| 70 × 70         | 84565        | 7.001734 |
| 75 × 75         | 96980        | 7.001917 |
| 80 × 80         | 110245       | 7.002160 |
| 85 × 85         | 124360       | 7.002191 |

Table 3. Grid sensitivity check using the variation of  $Nu$  with mesh elements for  $\phi = 0.05$ ,  $Ri = 1$ ,  $Re = 100$  and  $Gr = 10^4$ .

| Average Nusselt Number |              |                          |
|------------------------|--------------|--------------------------|
| Ri                     | Present Code | Abu-Nada and Chamkha [8] |
| 0.2                    | 2.781107     | 2.866557                 |
| 0.5                    | 2.328368     | 2.365185                 |
| 2                      | 1.743216     | 1.741458                 |
| 5                      | 1.459776     | 1.453406                 |

Table 4. Comparison of average Nusselt number from the present code with the results of Abu-Nada and Chamkha [8] for  $Gr = 100$  and  $\phi = 0.05$  (water- $Al_2O_3$  nanofluid).

### Code Validation

Due to lack of availability of experimental data for the present case, the computational code is validated with the results obtained for mixed convection flows in a lid-driven square enclosure with heated top wall and filled with water- $Al_2O_3$  nanofluid by Abu-Nada and Chamkha [8]. Table 4 shows the comparison of average Nusselt number of the hot wall for different Richardson numbers at  $Gr = 100$  and  $\phi = 0.05$  with that of Abu-Nada and Chamkha [8]. The agreement is found to be close enough which validates the present computations in terms of average Nusselt number. Therefore, it can be decided that the current code can be used to predict the characteristics of mixed convection heat transfer for the present problem quite accurately.

### Results and Discussions

The present investigation is carried out on pure mixed convection region at  $Ri = 1$  for both plain fluid (water) and nanofluid (water- $Al_2O_3$ ) containing 5% solid-volume fraction of nanoparticles. Reynolds number is varied from 0.1 to  $10^3$  at  $Ri = 1$  and thus Grashof number simultaneously changes from 0.01 to  $10^6$  with a view to understand the combined effect of  $Re$  and  $Gr$  on the nature of mixed convection inside a lid-driven trapezoidal enclosure. The limiting range of Reynolds number is selected based on the observation of average Nusselt number which shows the change of flow from laminar to chaos.

Figure 2 shows the effect of increasing both Reynolds and Grashof numbers on the average Nusselt number for the cases of  $\phi = 0$  and 0.05 at  $Ri = 1$ . It can be observed that the average Nusselt number along the bottom wall of the trapezoidal enclosure increases continuously with increasing  $Re$  and  $Gr$  simultaneously. However, three important distinct points can be observed from this figure. First, the transition from conduction to convection regime is noticed within the laminar zone. At  $Re \leq 3$  and  $Gr \leq 9$ , an imbalance between the superposed effects of conduction and incipient convection is reflected in a slow approach to the convective regime. This is because the average Nusselt number remains constant within this regime for both plain and nanofluid. The second and third observations are the beginning and the end of transition from laminar to chaos. Those are indicated by two points A (maximum  $Nu$ ) and B (minimum  $Nu$ ), respectively in figure 2. Within this region, a sudden but gradual drop of average Nusselt number from A to B is ob-

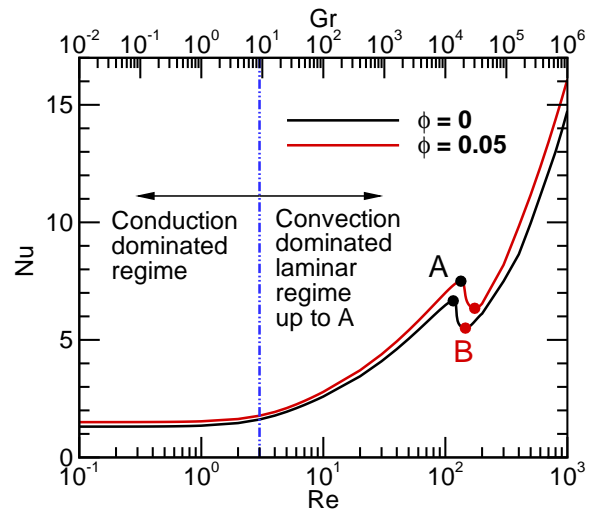


Figure 2. Combined effect of Reynolds and Grashof numbers on average Nusselt number of the heated wall for constant Richardson number,  $Ri = 1$ . Solid black line represents plain fluid whereas red line represents nanofluid with  $\phi = 0.05$ . Onset of laminar-chaos transition in mixed convection regime is clearly marked by two black and red points, A and B.

| Parameter          | $\phi = 0$ | $\phi = 0.05$ |
|--------------------|------------|---------------|
| $Re(A)$            | 116        | 134           |
| $Gr(A)$            | 13456      | 17956         |
| $Re(B)$            | 146        | 174           |
| $Gr(B)$            | 21316      | 30276         |
| $\Delta Nu(A - B)$ | 1.159668   | 1.1525785     |

Table 5. List of critical parameters for transition from laminar to chaos in the present problem.

served for both plain fluid and nanofluid. The summary of all critical parameters describing the characteristics of the transitional region is presented in table 5. It is interesting to note that the influence of increasing both Reynolds and Grashof numbers is overwhelmed here in the mixed convection flows. Moreover, the presence of nanofluid does not change the nature of this transition process. Average Nusselt number for all the fluids with higher solid-volume fractions indicates a slight shift in transitional value of  $Re$  and  $Gr$ , and the drop of  $Nu$  ( $\Delta Nu$ ) also slightly decreases with the presence of nanofluid. The reduction of heat transfer may be attributed by the drastic change of flow and thermal fields, and heat transfer mechanism. In order to explain the reason for drop in  $Nu$ , it is necessary to observe the structures in flow and thermal fields within the transition regime.

The variation of streamline and isotherm contours with both Reynolds and Grashof numbers where  $Ri = 1$  for plain fluid is depicted in figure 3. It is easily understood from these figures that at point A, buoyancy flow converges with core flow to form a single clockwise rotating cell of semicircular structure and thus indicates dominating flow field. A minor counter-clockwise rotating vortex is observed at the bottom right corner. Further increase of Reynolds and Grashof numbers from point A to point B reveals that the counter-clockwise cell at the bottom right corner starts to expand in size and thus with increasing strength opposes the circulating flow. Like streamlines, the isotherm contours show significant change with increasing  $Re$  and  $Gr$ . At  $Re = 116$ , the isotherm contours are clustered near the heated bottom wall, which indicate the existence of steep

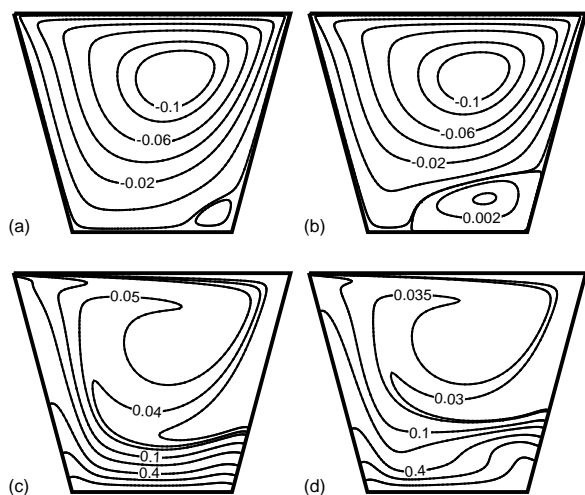


Figure 3. Streamlines (on the top) and isotherms (on the bottom) contours of the plain fluid ( $\phi = 0$ ) for (a), (c)  $Re = 116$  and (b), (d)  $Re = 146$  at  $Ri = 1$ .

temperature gradients and thin thermal boundary layers in the vertical direction. But when  $Re = 146$ , the temperature gradients close to the bottom wall and at the place of secondary developing vortex of the bottom right corner are less steep as compared to the case of  $Re = 116$ . The mixing of the cold and the hot fluids also becomes weak which further initiates the reduction of the conduction and convection modes of heat transfer inside the trapezoidal enclosure.

Figure 4 is dedicated for the purpose of comparing the presence of nanofluid on flow and temperature profiles in relation to the plain fluid. Apparently, it looks like the profiles of flow fields are unchanged, but the careful observation reveals that the size of the cell increases with increasing  $\phi$ , which corresponds to a faster flow field due to increased mechanical effect of the moving lid at higher  $Re$  (points A and B). Moreover, isothermal contours are comparatively more distorted for nanofluid and thus indicating better mixed convection heat transfer. Since  $Nu$  is always higher for nanofluid in compared with plain fluid, the resulting variation of critical parameters (values of  $Re$  and  $Gr$  at points A and B) is influenced by the improved thermo-physical properties of the nanofluid.

### Conclusions

The present study focuses on the phenomenon how pure mixed convection heat transfer at  $Ri = 1$  inside short base lid-driven trapezoidal enclosure changes with the variation of both  $Gr$  and  $Re$  and thus illustrates the change from laminar to chaos. Reynolds number is varied over a suitable range so that the transition from laminar to chaos region can be observed. Quantitative predictive criteria for the beginning and the end of transition are presented. It is found that both the flow and the temperature profiles are influenced by the combined effect of Reynolds and Grashof numbers to a great extent. The profiles also vary with the presence of nanofluid. The limit of critical parameters relating to the onset of the transition significantly depends on the presence of nanofluid as compared with plain fluid.

### Acknowledgements

The authors gratefully acknowledge the support provided by the Department of Mechanical Engineering, Bangladesh University of Engineering and Technology (BUET) during this research work.

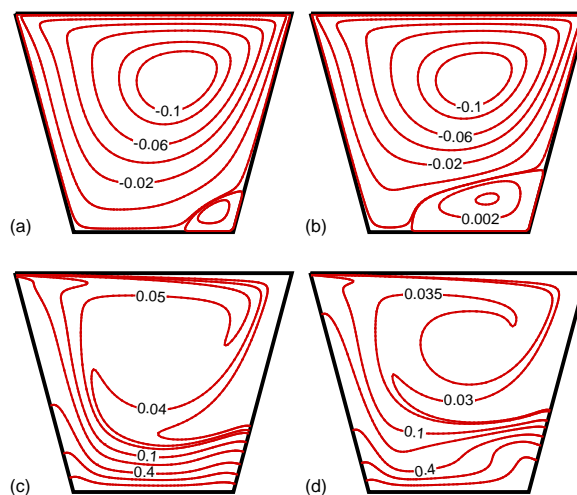


Figure 4. Streamlines (on the top) and isotherms (on the bottom) contours of the nanofluid ( $\phi = 0.05$ ) for (a), (c)  $Re = 134$  and (b), (d)  $Re = 174$  at  $Ri = 1$ .

### References

- [1] Stanish, M., Schajer, G. and Kayihan, F., A mathematical model of drying for hygroscopic porous media, *AIChE J.*, **32**, 1986, 1301–1311.
- [2] Pilkington, L., Review lecture. the float glass process, *Proceedings of the Royal Society of London. Series A, Mathematical and Physical Sciences*, **314**, 1969, 1–25.
- [3] Hossain, M. N., Mamun, M. A. H. and Saha, S., Mixed convection in a trapezoidal cavity with moving lid at top wall and heating from below, in *International Conference on Chemical Engineering*, Dhaka, Bangladesh, 2008.
- [4] Chowdhury, M. N. H., Saha, S. and Mamun, M. A. H., Mixed convection analysis in a lid driven trapezoidal cavity with isothermal heating at bottom for various aspect angles, in *8th International Conference on Mechanical Engineering*, Dhaka, Bangladesh, 2009.
- [5] Hasan, M. N., Saha, S., Saha, G. and Islam, M. Q., Effect of sidewall inclination angle of a lid-driven trapezoidal enclosure on mixed convective flow and heat transfer characteristics, in *13th Asian Congress of Fluid Mechanics*, Dhaka, Bangladesh, 2010.
- [6] Mamun, M. A. H., Tanim, T. R., Rahman, M. M., Saidur, R. and Nagata, S., Mixed convection analysis in trapezoidal cavity with a moving lid, *Int. J. Mech. Mater. Eng.*, **5**, 2010, 18–28.
- [7] Cheng, T., Characteristics of mixed convection heat transfer in a lid-driven square cavity with various richardson and prandtl numbers, *Int. J. Therm. Sci.*, **50**, 2011, 197 – 205.
- [8] Abu-Nada, E. and Chamkha, A. J., Mixed convection flow in a lid-driven inclined square enclosure filled with a nanofluid, *Euro. J. Mech. B/Fluids*, **29**, 2010, 472–482.
- [9] Zienkiewicz, O. C. and Taylor, R. L., *The finite element method*, volume 1, 1973.